

SPECIAL ISSUE: REVIEW

Behaviors of quenched polyampholytes in solution and gel state

Sarkyt E. Kudaibergenov^{1,2}  | Oguz Okay³ 

¹Laboratory of Engineering Profile, Satbayev University, Almaty, Republic of Kazakhstan

²Department of Functional Polymers, Institute of Polymer Materials and Technology, Almaty, Republic of Kazakhstan

³Department of Chemistry, Istanbul Technical University, Istanbul, Turkey

Correspondence

Sarkyt E. Kudaibergenov, Institute of Polymer Materials and Technology, Microregion "Atyrau 1," Bld.3/1, Almaty 050019, Republic of Kazakhstan.
Email: skudai@mail.ru

Oguz Okay, Department of Chemistry, Istanbul Technical University, Maslak, 34469 Istanbul, Turkey.
Email: okayo@itu.edu.tr

Funding information

Ministry of Education and Science of the Republic of Kazakhstan, Grant/Award Number: IRN AP08855552; Türkiye Bilimler Akademisi, Grant/Award Number: Full member 2020

The quenched or strongly charged polyampholytes represent amphoteric macromolecules consisting of static positive and negative charges that slightly depend on pH. Here, the behavior of linear and cross-linked quenched polyampholytes (QPA) in aqueous salt solutions is reviewed together with their stimuli-responsive character as functions of temperature and ionic strength. The volume-phase, swelling-deswelling, self-healing, viscoelastic, and mechanical properties of QPA gels are also discussed. Complexation of QPA with dye molecules, surfactants, and proteins is outlined. Application aspects of QPA cover biotechnology, biomedicine, oil recovery, desalination, etc.

KEYWORDS

core-shell structure, hydrogels, quenched polyampholytes, solution properties, stimuli-sensitivity

1 | INTRODUCTION

Linear and cross-linked quenched polyampholytes (QPA) exhibit salt-tolerant,¹ thermal-resistant,² shear-stable,² self-healing,³⁻⁵ antifouling,^{6,7} self-assembling,⁸⁻¹¹ and stimuli-responsive,¹²⁻¹⁴ properties that provide broad impact as enhanced oil recovery (EOR),^{15,16} and drag reduction agents,^{17,18} structural biomaterials,¹⁹ controlled delivery systems,^{20,21} energy storage devices,²² supercapacitors,²³ and actuators.²⁴ Synthetic protocol of QPA includes the conventional free-radical copolymerization (FRP) of charged monomers,^{1,25-32} polymerization in microemulsion,³³⁻³⁹

polymerization of anionic-cationic monomer pairs without counterions,⁴⁰ or zwitterionic monomers,⁴¹ and reversible addition-fragmentation chain transfer (RAFT) polymerization.^{7,14,42,43} The QPA prepared in solution have a tendency to alternate between positively- and negatively-charged monomers while prepared by means of a microemulsion polymerization allows to produce very high molecular weight copolymers (up to 1×10^7 g mol⁻¹) that are more homogeneous in composition, with a reduced probability of continuous sequences of monomers of the same charge in the macromolecular chain. The RAFT controlled radical polymerization technique produces both random and block copolymers with low molecular weight and narrow polydispersity index (PDI).

The electrostatic interactions between charged monomeric units of polyampholytes are of primary interest because their solution properties depend on the charge density, charge balance, charge spacing, and distribution, as well as on the ionic strength of the solution adjusted by low-molecular-weight salts. In this context, the nature of the salts following the Hoffmeister series can determine the conformation and hydrodynamic size of QPA as a function of

Abbreviations: AAm, Acrylamide; AMPDAC, 2-Acrylamido-2-methylpropyldimethylammonium chloride; AMPS, Sodium salt of 2-acrylamido-2-methylpropanesulfonate; APTAC, 3-Acrylamidopropyltrimethylammonium chloride; C18A, n-Octadecyl acrylate; CAA, 2-carboxyethylacrylate; DMAEA-Q, Quaternized N,N-dimethylaminoethylacrylate; DOAC, N,N-Dimethyloctadecyl allyl ammonium chloride; MAA, Methacrylic acid; MADQUAT, 2-(Methacryloyloxy)ethyltrimethylammonium chloride; MAPTAC, [3-(Methacryloylamino)propyl]trimethylammonium chloride; METMAC, [2-(Methacryloyloxy)ethyl]trimethylammonium chloride; NaSS, Sodium 4-vinylbenzenesulfonate; SPMA, 3-Sulfopropylmethacrylate; SSS, Sodium styrene sulfonate; TEGDMA, Triethyleneglycoldimethacrylate; TMA, [2-(Acryloyloxy)ethyl]trimethylammonium chloride; VBTAC, N-Vinylbenzyltrimethylammonium chloride.

ionic strength.⁴⁴ Another specific property of QPA is the anti-polyelectrolyte effect in response to salt addition.²⁵⁻²⁷ Charge-balanced and charge-unbalanced QPA consisting of a core (polyampholyte regime) and shell (polyelectrolyte regime) structure show antagonism in aqueous salt solutions.^{45,46} Addition of low-molecular-weight salts tends to shrink the shell part and to swell the core part. Such antagonism between polyelectrolyte (shell) and polyampholyte (core) effects can take place at relatively high ionic strengths. According to the literature survey, QPA are less studied subject in comparison with annealed polyampholytes,⁴⁷⁻⁴⁹ and polymeric betaines.⁵⁰ Polyzwitterions based on carbo-, sulfo-, and phosphobetaines are not included in this review and discussed only in a special case when they are compared with QPA.

2 | PROPERTIES OF QUENCHED POLYAMPHOLYTES IN WATER AND AQUEOUS-SALT SOLUTIONS

Dilute solution properties of copolymers of 2-acrylamido-2-methylpropyldimethylammonium chloride (AMPDAC) and sodium salt of 2-acrylamido-2-methylpropanesulfonate (AMPS) have been studied as functions of copolymer composition, temperature, time, pH, and added low-molecular-weight electrolytes.²⁵⁻²⁹ Equimolar copolymers display a minimal viscosity in pure water and a maximal one in concentrated salt solutions. As the copolymer compositions deviate from an equimolar, charge imbalances increase the hydrodynamic volume of macromolecules. Candau et al studied aqueous-salt solution properties of high charge density polyampholytes derived from 2-methacryloyloxyethyltrimethylammonium chloride (METMAC) and AMPS.³³⁻³⁷ Solubility and viscometry experiments show that the solution behavior of METMAC-AMPS copolymers is essentially controlled by two parameters, namely, the net effective charge fixed by the copolymer composition, and the ionic strength. Copolymers with a strong net charge behave more like polyelectrolytes. At intermediate copolymer compositions, the behavior depends on the duality between repulsive (polyelectrolyte effect) and attractive (polyampholyte effect) electrostatic interactions. Depending on the ionic strength, either one of these antagonist effects will dominate. The same authors also reported solution properties of low charge density METMAC-AMPS polyampholytes with incorporated acrylamide (AAm) monomer units.³⁶ At a low salt concentration (C_s), attractive electrostatic interactions are dominant and hence METMAC-AAm-AMPS chains collapse. At a high C_s , when the Debye-Huckel length becomes short enough that the Coulomb interactions are screened out, then the excluded volume interactions are dominant and the terpolymer has a swollen or Gaussian conformation, depending on the quality of the solvent. Below a critical value of C_s , the chains with zero or small net charge precipitate due to the polyampholyte effect. Note that the mass polydispersity can also play a considerable role since the collapse-swollen transition is very sensitive to the molecular weight of the polyampholyte.⁵¹ Everaers et al⁵² discussed multichain effects in polyampholyte solutions of finite concentration and found that the

existing single-chain theories are limited to exponentially small concentrations, if the sample contains net charges of both signs. It has been shown that QPA have a strong tendency to form neutral complexes and to precipitate.

Solution properties of equimolar QPA prepared from AMPS and 3-acrylamidopropyltrimethylammonium chloride (APTAC) via RAFT and conventional free-radical polymerization (FRP) were compared with stoichiometric polyelectrolyte complexes (SPEC) obtained from anionic and cationic polyelectrolyte pairs, for example, PAMPS and PAPTAC (Figure 1).⁴² The average molecular mass of $P(\text{AMPS-APTAC})_{\text{FRP}}$ was 724 times higher than that of $P(\text{AMPS-APTAC})_{\text{RAFT}}$. The PDI of $P(\text{AMPS-APTAC})_{\text{RAFT}}$ was narrow and in the range of 1.14 to 1.44 whereas the PDI of $P(\text{AMPS-APTAC})_{\text{FRP}}$ was broad and equal to 16.2. In pure water, the mixture of PAMPS and PAPTAC precipitates while QPA obtained by FRP is turbid, and QPA prepared by RAFT is water-soluble. The reason is that in pure water the $(\text{PAMPS-PAPTAC})_{\text{SPEC}}$ is stoichiometrically charge-neutralized and becomes fully hydrophobic while $P(\text{AMPS-APTAC})_{\text{FRP}}$ forms large aggregates stabilized by continuous sequences (microblocks) of oppositely charged monomers. However, such colloidal aggregates are prevented from precipitation and preserved in aqueous solution by "loops" and "dangles" consisting of cationic and anionic monomers. In case of $P(\text{AMPS-APTAC})_{\text{RAFT}}$ the probability of formation of interionic aggregates ($N_{\text{agg}} = 2-3$) between oppositely charged monomers is minimal because the pendant sulfonate anions and quaternary ammonium cations are randomly distributed and the molecular weights of polymers prepared by RAFT are low. In this context, it would be interesting to determine the critical molecular mass of QPA that is transformed from molecular dispersion to colloidal solution. In aqueous NaCl, both $P(\text{AMPS-APTAC})_{\text{RAFT}}$ and $P(\text{AMPS-APTAC})_{\text{FRP}}$ adopt unimer state due to the screening of electrostatic interactions by low-molecular-weight anions and cations. The turbidity of $P(\text{AMPS-APTAC})_{\text{FRP}}$ with high molecular mass disappears in aqueous solutions of NaCl. The values of hydrodynamic radius (R_h), light scattering intensity (LSI), and zeta-potential (ζ) of $P(\text{AMPS-APTAC})_{\text{RAFT}}$ and $P(\text{AMPS-APTAC})_{\text{FRP}}$ depend on the NaCl concentration. In aqueous solutions of NaCl ($C_s = 0.01-2.0$ M) the values of R_h are in the range of 2.7 to 4.8 nm for $P(\text{AMPS-APTAC})_{\text{RAFT}}$ while R_h and LSI of $P(\text{AMPS-APTAC})_{\text{FRP}}$ decreased with an increase of NaCl concentration up to 0.1 M. The zeta-potential for both $P(\text{AMPS-APTAC})_{\text{RAFT}}$ and $P(\text{AMPS-APTAC})_{\text{FRP}}$ are close to zero irrespective of NaCl concentration. This is due to the complete neutralization of sulfonate anions and quaternary ammonium cations of macromolecules.

The behavior of diblock QPA composed of anionic PAMPS and cationic PAPTAC blocks was studied in water and aqueous-salt solutions.¹³ They were abbreviated as $\text{PAMPS}_{82}\text{-PAPTAC}_n$, where the subscript indicates the degree of polymerization, and $n = 37, 83,$ and 181 . It was shown that the equimolar $\text{PAMPS}_{82}\text{-PAPTAC}_{83}$ precipitates in pure water due to the formation of intra-polyelectrolyte complexes (intra-PEC) between anionic and cationic blocks while $\text{PAMPS}_{82}\text{-PAPTAC}_{37}$ and $\text{PAMPS}_{82}\text{-PAPTAC}_{181}$ containing an excess of anionic and cationic blocks, respectively, are fully water-soluble. It is supposed that the equal numbers of oppositely charged PAMPS

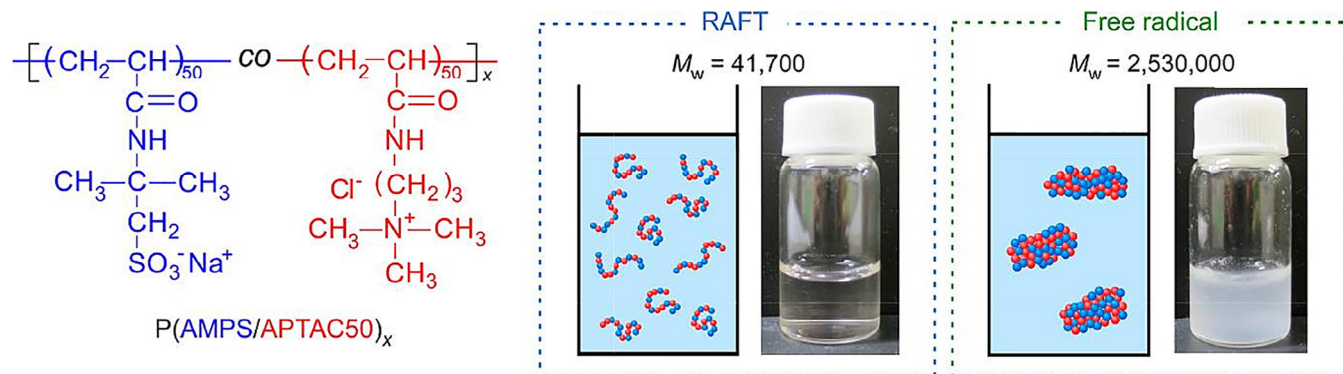


FIGURE 1 Repeated monomeric units of AMPS-co-APTAC, and images of QPA prepared via RAFT and conventional free-radical polymerization. Reproduced from Reference 42 with permission from the American Chemical Society [Colour figure can be viewed at wileyonlinelibrary.com]

and PAPTAC blocks are involved into formation of a “core,” while the excess of PAMPS and PAPTAC blocks are replaced in a “shell.” It is interesting to compare the behaviors of diblock PAMPS₈₂-PAPTAC_n copolymers with random QPA based on of AMPS_m-co-APTAC_n in aqueous-salt solutions, where $m = 25, 50,$ and 75 mol%, $n = 75, 50,$ and 25 mol%.^{46,47} Equimolar or balanced QPA prepared by RAFT and FRP are insoluble in pure water but dissolved in saline water. The non-equimolar or unbalanced QPA, to whom belong PAMPS₈₂-PAPTAC₃₇ and PAMPS₈₂-PAPTAC₁₈₁ synthesized by RAFT, and AMPS₂₅-co-APTAC₇₅ and AMPS₇₅-co-APTAC₂₅ prepared by FRP are fully water-soluble. In aqueous solutions, the zeta potentials of PAMPS₈₂-PAPTAC₃₇ and PAMPS₈₂-PAPTAC₁₈₁ are equal to -15.6 and $+22.8$ mV, respectively. The zeta-potentials of AMPS₂₅-co-APTAC₇₅ and AMPS₇₅-co-APTAC₂₅ are correspondingly positive ($\zeta = +50$ mV) and negative ($\zeta = -40$ mV) while the balanced QPA PAMPS₈₂-PAPTAC₈₃ and AMPS₅₀-co-APTAC₅₀ are in electroneutral state ($\zeta = 0$). Different behavior of unbalanced and balanced QPA upon increasing the ionic strength is illustrated in Figure 2. Increasing the ionic strength screens the electrostatic repulsion between uniformly charged groups, or shields the electrostatic attraction between oppositely charged monomers depending on the domination of polyelectrolyte or polyampholyte effects, respectively (Table 1). In the former case, the macromolecular chain contracts, whereas in the latter case it expands.

In aqueous KCl solutions, the intrinsic viscosities of AMPS₂₅-co-APTAC₇₅ and AMPS₇₅-co-APTAC₂₅ decrease while the intrinsic viscosity of AMPS₅₀-co-APTAC₅₀ increases demonstrating *anti-polyelectrolyte* behavior. Addition of low-molecular-weight salts to AMPS₅₀-co-APTAC₅₀ shields the electrostatic attraction between the oppositely charges and results in increasing the intrinsic viscosity. In aqueous solution, the conformation of unbalanced PAMPS₈₂-PAPTAC₃₇, PAMPS₈₂-PAPTAC₁₈₁, AMPS₂₅-co-APTAC₇₅, and AMPS₇₅-co-APTAC₂₅ has a core-shell structure where the core and shell parts exist in polyampholyte and polyelectrolyte regimes, respectively. Addition of low-molecular-weight salts tends to shrink the shell part and to swell the core part. Such antagonism may cause competition between polyelectrolyte (shell) and polyampholyte (core) effects at relatively high ionic strengths.

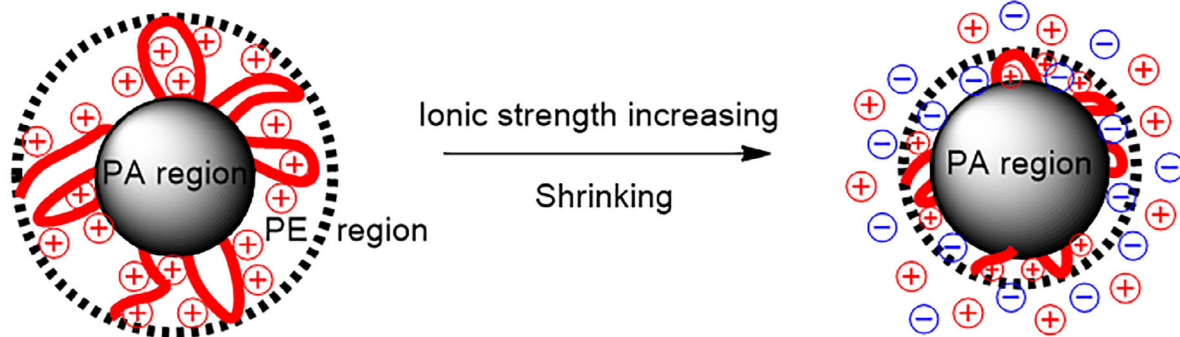
All three QPA, namely PAMPS₈₂-PAPTAC₃₇, PAMPS₈₂-PAPTAC₁₈₁, and PAMPS₈₂-PAPTAC₈₃ exhibit thermo-responsive character with a lower critical solution temperature (LCST) at definite polymer (C_p) and NaCl concentrations. Phase transitions for PAMPS₈₂-PAPTAC₈₃, PAMPS₈₂-PAPTAC₃₇ and PAMPS₈₂-PAPTAC₁₈₁ are observed for $[\text{NaCl}] = 0.5\text{--}0.75, 0.8\text{--}1.1,$ and $0.7\text{--}0.9$ M, respectively. The phase transition temperature of PAMPS₈₂-PAPTAC₈₃ in 0.9 M NaCl shifts toward higher values with decreasing C_p from 10 to 1 g L⁻¹.

A series of charge-balanced or equimolar QPA from cationic N-vinylbenzyltrimethylammonium chloride (VBTAAC) and anionic sodium 4-vinylbenzenesulfonate (NaSS) monomers were prepared via RAFT polymerization with different degree of polymerization (Figure 3).¹³ By measurements of the turbidity (%T), hydrodynamic radius (R_h), LSI, optical microscopy (OM), and fluorescence probe (FP), it was shown that the UCST of QPA is shifted to higher temperature with a decrease in NaCl concentration, or with an increase in polymer concentration (C_p) or the degree of polymerization. Table 2 summarizes the theoretically calculated M_n , PDI, R_h , and zeta-potential ζ of P(VBTAAC-NaSS)₂₀ and P(VBTAAC-NaSS)₉₇ in 0.1 and 1.0 M NaCl at 70°C , where the subscripts denote the degree of polymerization. Such small R_h values indicate that in aqueous-salt solutions the polymers above the UCST exist in unimer states.

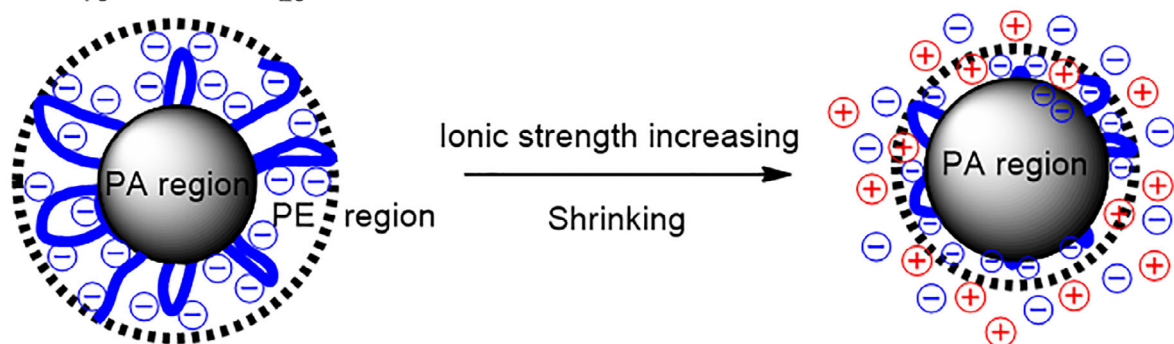
Formation of spherical globules with a radius of gyration R_g of around 2.5 nm was directly visualized by Field Emission Scanning Electron Microscope (FE-SEM) images for charge-balanced polyampholyte hydrogels made of NaSS and [3-(methacryloylamino)propyl]trimethylammonium chloride (MAPTAC) denoted as poly(NaSS-co-MAPTAC) (Figure 4A).^{53,54} The polymer consists of spherical globules forming polymer-rich domains, polymer-poor interglobular regions and clusters (Figure 4B). Thus the existence of globular structure for QPA irrespective of the solution or gel state is in good agreement with theoretical predictions.^{51,52,55,56}

The zeta-potential values of P(VBTAAC-NaSS)₂₀ and P(VBTAAC-NaSS)₉₇ above the UCST are close to zero and in favor of the electroneutrality of QPA. The polarity of the hydrophobic domains formed by P(VBTAAC-NaSS)_n below and above the UCST was evaluated with the help of fluorescent probe peptide nucleic acid (PNA). The most

AMPS₂₅-co-APTAC₇₅, Z = +50



AMPS₇₅-co-APTAC₂₅, Z = -40



AMPS₅₀-co-APTAC₅₀, Z = 0

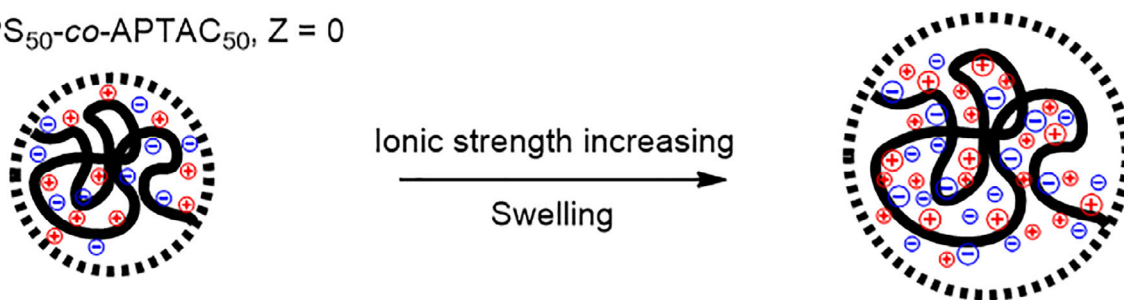


FIGURE 2 Schematic representation of a core-shell structure, and the behavior of QPA in aqueous-salt solutions. Reproduced from Reference 45 with permission from Bulletin of Karaganda University [Colour figure can be viewed at wileyonlinelibrary.com]

Copolymers	Ionic strength, KCl/M					
	0	0.05	0.1	0.5	0.75	1.0
AMPS ₂₅ -co-APTAC ₇₅	46.4 (0.5)	-	2.7 (0.1)	-	2.3 (0.1)	1.1 (0.1)
AMPS ₅₀ -co-APTAC ₅₀	-	0.9 (0.1)	1.4 (0.1)	2.2 (0.1)	1.9 (0.1)	2.0 (0.1)
AMPS ₇₅ -co-APTAC ₂₅	53.8 (0.5)	-	2.9 (0.1)	-	2.4 (0.1)	1.5 (0.1)

Note: The standard deviations are given in parenthesis.

TABLE 1 Intrinsic viscosities, in dL g⁻¹, of AMPS_m-co-APTAC_n copolymers at various ionic strengths

commonly used luminescent labels to evaluate the microenvironment and conformational transitions of charged macromolecules are pyrene and naphthalene. However, they do not possess any stimuli-

responsive character. In contrast, a series of quinoline-labeled QPA composed of AMPS and MAPTAC exhibit pH-controlled color change that is tuned by macromolecular charge.⁵⁷

Anionic diblock copolymer (AMPS₅₀-*b*-APTAC₅₀)₉₁-(AMPS)₆₇ and cationic diblock copolymer (AMPS₅₀-*b*-APTAC₅₀)₉₁-(APTAC)₈₈ represent the charge-balanced QPA surrounded by either anionic or cationic blocks (Figure 5).⁵⁸ One can suppose that the core of such copolymers composed of cationic and anionic monomers

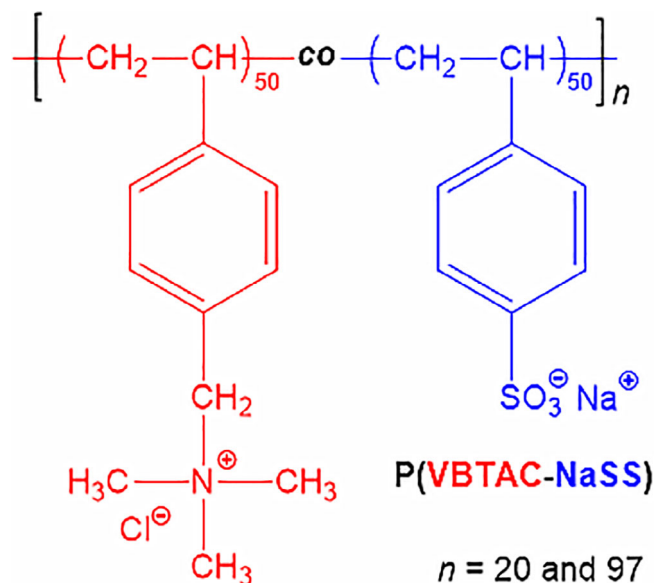


FIGURE 3 Chemical structure of statistical P(VBTAC-NaSS)_n copolymer. Redrawn from Reference 13 with permission from MDPI [Colour figure can be viewed at wileyonlinelibrary.com]

TABLE 2 The values of M_n , PDI, R_h , ζ of P(VBTAC-NaSS)₂₀ and P(VBTAC-NaSS)₉₇ at $C_p = 2.0 \text{ g L}^{-1}$ and 70°C

Samples	$M_n \cdot 10^{-3}$ (theory)	PDI	R_h , nm	ζ , mV
0.1 M NaCl P(VBTAC-NaSS) ₂₀	4.2 (0.1)	0.12 (0.02)	2.4 (0.1)	-0.32 (0.02)
1.0 M NaCl P(VBTAC-NaSS) ₉₇	20 (1)	0.21 (0.02)	3.7 (0.1)	+0.53 (0.02)

Note: The standard deviations are given in parenthesis.

(polyampholyte regime) forms intra-PEC while the shell part bears the excess of either positive or negative charges (polyelectrolyte regime).

The behavior of hydrophobically modified QPA is different from ordinary QPA. Introduction of the hydrophobic cationic monomer N,N-dimethyloctadecyl allyl ammonium chloride (DOAC) and the anionic sodium styrene sulfonate (SSS) monomer together with non-ionic AAm into macromolecular chain leads to self-assembling accompanied by intra- and intermacromolecular associates in dependence of critical association concentration (CAC) that is around 0.165 to 0.190 wt% (Figure 6).⁸ Environmental scanning electron microscope (ESEM) images of DOAC-SSS-AAm copolymer solutions at below CAC show that the network structure has sparse and scattered nature due to formation of intramacromolecular aggregates, while above CAC, it has a dense honeycomb structure stabilized by intermacromolecular hydrophobic association. Thus, the copolymer solution at below and above CAC has a low and high apparent viscosity, respectively. In aqueous-salt solutions, the apparent viscosity of the solution increases demonstrating the antipolyelectrolyte character. The salt-, temperature-, and shearing resistance of DOAC-SSS-AAm copolymers suggest this hydrophobically-modified QPA applicable for EOR.

3 | BEHAVIOR OF QUENCHED POLYAMPHOLYTE GELS

Understanding the structure, swelling, and collapsing of hydrogels based on QPA as a function of the copolymer composition, microstructure,

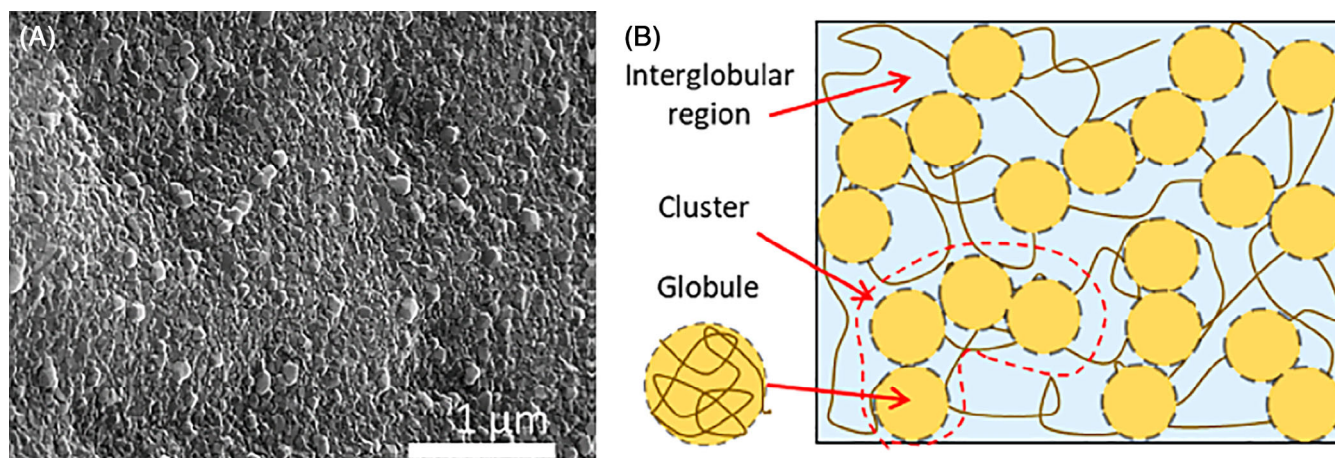


FIGURE 4 Cross-sectional FE-SEM image (A), and a scheme representing the microstructure of poly(NaSS-co-MPTC) (B). Reproduced from Reference 53 with permission from the American Chemical Society [Colour figure can be viewed at wileyonlinelibrary.com]

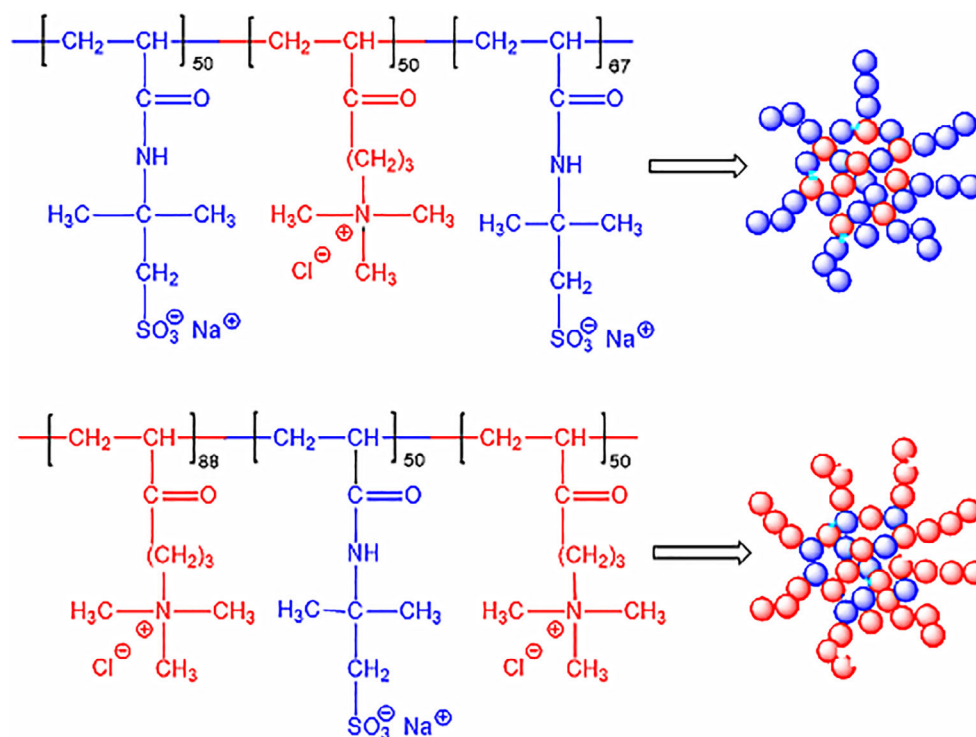


FIGURE 5 Chemical structure and speculative conformation of anionic diblock (AMPS₅₀-*b*-APTAC₅₀)₉₁-(AMPS)₆₇ and cationic diblock (AMPS₅₀-*b*-APTAC₅₀)₉₁-(APTAC)₈₈ copolymers. Redrawn from Reference 58 with permission from MDPI [Colour figure can be viewed at wileyonlinelibrary.com]

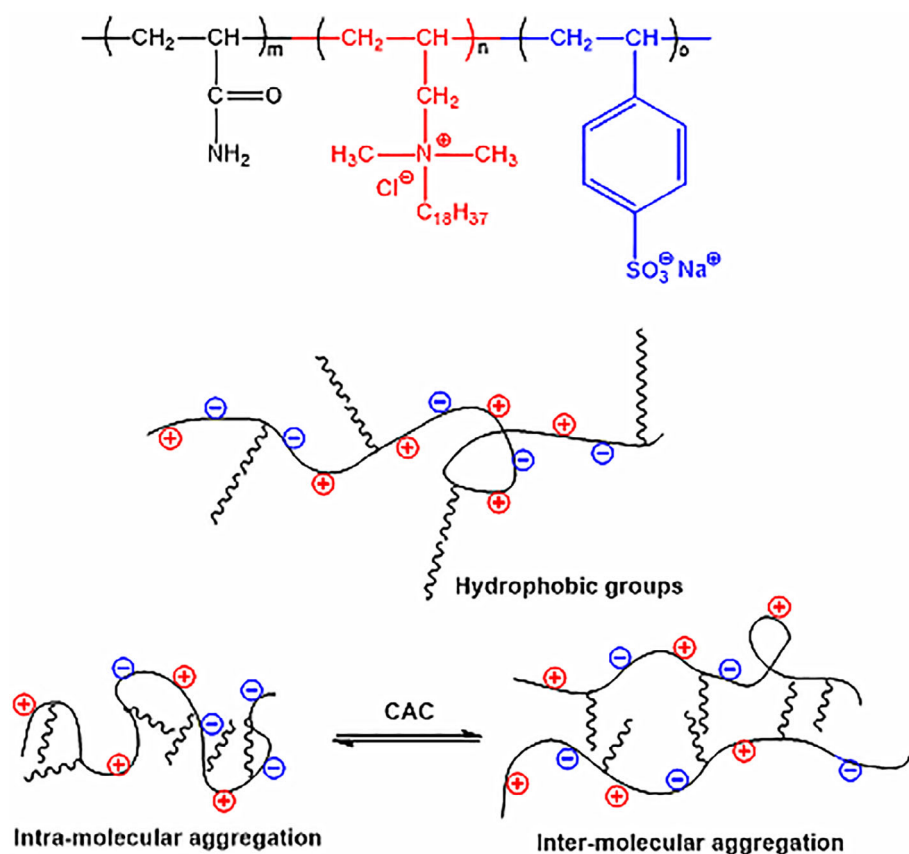


FIGURE 6 Structure of hydrophobic DOAC-SSS-AAm and its self-assembly. Redrawn from Reference 8 with permission from the Royal Society of Chemistry [Colour figure can be viewed at wileyonlinelibrary.com]

temperature, and ionic strength of aqueous solution will provide the development of a novel class of networks that possess the stimuli-responsive character, self-healing ability, strong adhesion, and

mechanical flexibility.⁵⁹ The long-range Coulombic interactions between opposite charges along the backbone is a governing factor of conformational and volume-phase changes of QPA hydrogels. Figure 7A shows

the equilibrium swelling ratio Q_e of QPA gels prepared by FRP of 2-(methacryloyloxy)ethyltrimethylammonium chloride (MADQUAT) and AMPS in pure water and 2 M NaCl solution.³⁹ Similar to linear QPA, hydrogels of QPA are in swollen and collapsed states depending on the net charge expressed as $f = f^+ - f^-$, where f^+ and f^- are the molar ratios of cationic and anionic monomers to the total monomer concentration, respectively. As the concentration of the anionic and cationic parts deviates from the equimolar ones, $f \neq 0$, the swelling ratio increases rapidly due to the increase of osmotically active ions in the hydrogel (Figure 7A). As the molar ratio of cationic to anionic groups approaches to unity, the excess free counterions that are not needed to satisfy the electro-neutrality of the chain are effectively "dialyzed" from the hydrogel interior. In 2 M NaCl solution, the electrostatic effects are screened and the swelling ratio Q_e levels off and hydrogel behaves as a neutral system. At a low ionic strength, polyampholyte chains bearing net charges of opposite signs form intraionic complexes leading to a phase separation. At a high ionic strength, the gel swells due to screening of electrostatic interactions leading to dissolution of such microscale structure, as schematic illustrated in Figure 7B.

QPA hydrogels based on MAPTAC-*co*-NaSS and AMPS-*co*-APTAC were compared with a polyion complex (PIC) composed of PMAPTAC and PNaSS as well as with a polyelectrolyte linear polymer poly(3-[(2-acrylamido)ethyl]dimethylammonio]propanesulfonate) (PAEDAPS) and hydrogel prepared from zwitterionic monomer [(2-methacryloyloxy)ethyl]dimethyl-(3-sulfopropyl)ammonium (polySBA) (Figure 8).^{44,60,61} The main difference between MAPTAC-*co*-NaSS and PMAPTAC-PNaSS hydrogels is that the former is composed of oppositely charged monomers while the latter is the product of matrix polymerization of NaSS on the matrix of PMAPTAC. The conformation of MAPTAC-*co*-NaSS can be stabilized by both inter- and intra-ionic interactions, while PMAPTAC-PNaSS chains are stabilized

by interionic salt bonds. In the case of polyelectrolyte polymers such as PAEDAPS and polySBA hydrogels, both intra- and interionic salt bonds can be realized. Both QPA and PIC do not contain the cross-linking agents and hence belong to the group of physical hydrogels which are formed at charge-balanced composition of monomers $f^+ = f^- = 0.5$, or at stoichiometric composition (1:1) of oppositely charged polyelectrolytes. In recent years, the main attention was focused on the physical QPA and PIC hydrogels with charge-balanced composition.⁶⁰ The effects of charge ratio and monomer concentration, as well as the molecular weight of polyelectrolytes on the swelling, toughness, self-healing, and viscoelasticity of QPA and PIC hydrogels were comparatively studied. It was demonstrated that the PIC hydrogels are much tougher than the QPA hydrogels and exhibit better mechanical properties. This is due to the structural and morphological differences between the two systems. The PIC hydrogel shows a more inhomogeneous, large segregated structure with large pore sizes (0.5–3.0 μm), while the QPA hydrogel shows a more homogeneous structure with pores of 0.1–0.3 μm in diameter.

The swelling properties of AMPS-*co*-APTAC and polySBA as a function of ionic strength were evaluated by continuous monitoring of 60 μm sized hydrogels using a fiber-optic based instrument.⁶² It was shown that both charge-balanced AMPS-*co*-APTAC and zwitterionic polySBA hydrogels exponentially swell upon increasing the ionic strength from 5×10^{-4} to 0.15 M NaCl. The swelling degree is higher for increased mol% of AMPS-*co*-APTAC and the charge density of the zwitterionic hydrogel polySBA. Thus, both charge-balanced QPA and zwitterionic polybetaines exhibit antipolyelectrolyte effect in response to added salts.⁶³ A reasonable explanation of this phenomenon is as follows: The opposite charges within QPA and zwitterionic hydrogels act as physical cross-links stabilized by inter- or intra-ionic contacts. Exponential swelling of AMPS-*co*-APTAC and polySBA with

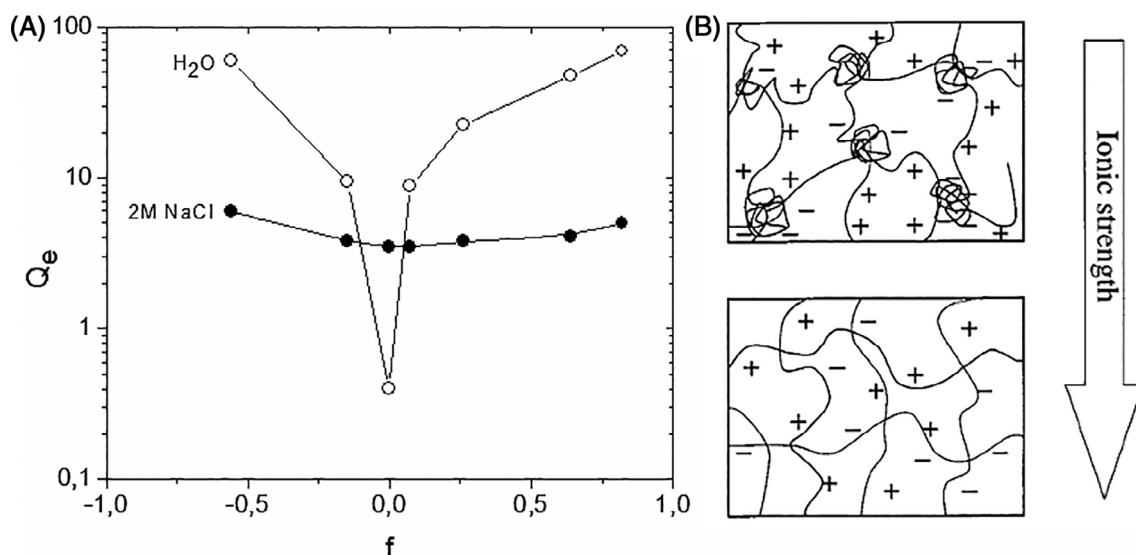


FIGURE 7 (A) Equilibrium swelling ratio Q_e as a function of the net charge for MADQUAT-AMPS in pure water and 2 M NaCl solution. Redrawn from Reference 39 with permission from the American Chemical Society. (B) Schematic representation of the internal structure of the gels in pure water (upper panel) and in response to increasing salt concentration (bottom panel). Reproduced from Reference 39 with permission from the American Chemical Society

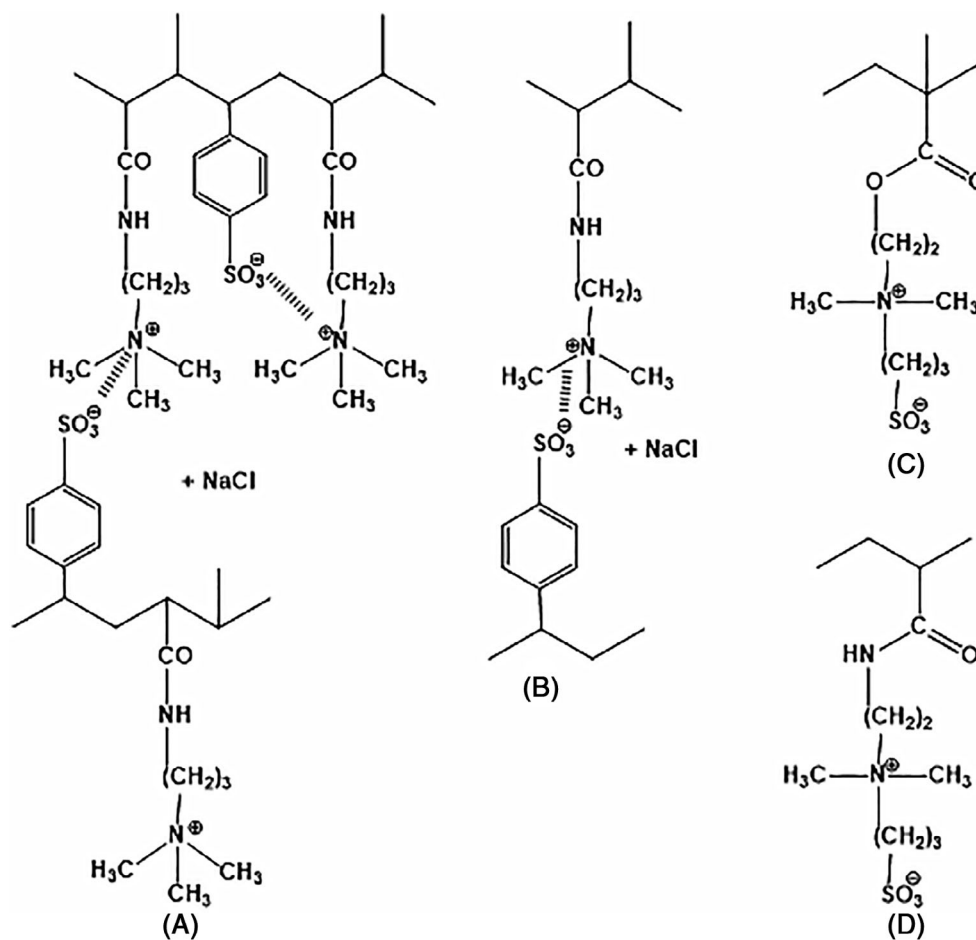


FIGURE 8 The structure of repeat units of MAPTAC-co-NaSS involved into intra- and interionic complexes (A), PMAPTAC-PNaSS complex (B), polySBA (C), and PAEDAPS (D)

an increase in the ionic strength is due to screening of the electrostatic attractions between opposite charges that diminishes both charge and crosslink density to contribute to swelling. The higher swelling degree of QPA hydrogel compared to zwitterionic hydrogel is the result of a larger number of cross-links in QPA hydrogels. The swelling properties of polyampholytic and polyzwitterionic hydrogels with anionic and cationic offsets represent typical polyelectrolyte character.

A new class of tough, viscoelastic, and self-healing QPA hydrogels was designed by Gong et al.^{3-5,64} They were prepared supramolecular QPA hydrogels by random copolymerization of oppositely charged ionic monomers at a high monomer concentration and equimolar monomer ratio (charge balance point). It was shown that the physical gels contain strong ionic bonds that play the role of permanent cross-links, and weak ionic bonds that are responsible for energy dissipation providing a high stretchability, twisting, fatigue resistance, internal friction, adhesion, self-healing, shape memory, anti-biofouling, and other important functions. In spite of topological difference, the QPA hydrogels are similar to the double-network hydrogels.⁶⁴ In both cases, the strong bonds form a primary network and the weak bonds form a sacrificial network. The volume swelling ratio, Young's modulus E , and the compressive fracture stress of P(MAPTAC-co-NaSS) hydrogels show peaks when plotted as a function of the net charge f .¹⁹ The peak positions correspond to the vicinity of charge balance point

($f \approx 0.48-0.53$) where the Coulomb attraction prevails over the repulsion, and the polymer chains collapse to a globular state. In imbalanced region ($f < 0.48$ and $f > 0.53$) the Coulomb repulsion prevails and polymer segments elongate. The shrinking of the gels near the charge balance point ($f \approx 0.505 \pm 0.025$) is accompanied by a dramatic increase in the modulus and fracture stress. It should be noted that dialysis of as-prepared hydrogel samples in pure water plays a crucial role in enhancing the ionic bond formation whereupon the polymer concentration governs the competition between intra-chain and inter-chain complexation to form a tough hydrogel.¹⁹

A series of experiments were carried out to clarify the effect of specific ions on mechanical and electrical properties of QPA hydrogels based on P(NaSS-co-MAPTAC) immersed in aqueous solutions of various salts.²² It was shown that the specific effects of low-molecular-weight salts can be categorized into three types, namely, charge screening, ion-pair formation, and ion interference with the hydration layer. The effects of the type and concentration of salts on the swelling capacity of QPA P (NaSS-co-MAPTAC),²² and hydrodynamic radius R_h of polyzwitterions (PAEDAPS)⁴⁴ are similar and can be interpreted in terms of Hoffmeister series for cations, $\text{Ca}^{2+} > \text{Mg}^{2+} > \text{K}^+ > \text{Na}^+ > \text{NH}_4^+ > \text{Li}^+$ having common anion (Cl^-), and for anions, $\text{SO}_4^{2-} > \text{Cl}^- > \text{Br}^- > \text{NO}_3^- > \text{ClO}_4^- > \text{SCN}^-$ having common cation (Na^+). This series correlates with affinities of water to different ionic species. The conceptual approach of Delgado et al.⁴⁴ concerning solution behavior of polyzwitterions in dependence of

salt concentration, salt type, and temperature considerably expands our understanding of chain conformation of this class of polymers and may be useful for interpretation of the behavior of QPA hydrogels. The attention should be paid to the mechanism of elongation of hydrogel samples upon stretching. One can suppose that the conformation of QPA consists of quasi-permanent cross-linking points (entangled chains) and globular structures similar to those shown in Figure 4B. Upon stretching the globular part stabilized by weak bonds unfolds and becomes extended.

Thermally-healable, hydrophobically modified physical QPA hydrogels based on oppositely charged AMPS and APTAC monomers have recently been prepared via micellar polymerization in the absence of a chemical cross-linker.⁶⁵ The micellar polymerization is a simple technique for preparing copolymers composed of hydrophilic and hydrophobic blocks.^{66–68} This technique bases on the copolymerization of a hydrophobic monomer such as *n*-octadecyl acrylate (C18A) solubilized within the surfactant micelles with a hydrophilic monomer in aqueous solutions by free-radical mechanism. Hydrophobically

modified QPA hydrogels were prepared via micellar copolymerization of an equimolar AMPS and APTAC monomer mixture in the presence of C18A in an aqueous SDS-NaCl solution that forms worm-like SDS micelles able to solubilize C18A monomer.⁶⁵ The resulting hydrogels have mixed micelles composed of SDS and C18A units interconnected by AMPS/APTAC copolymer chains, as schematically illustrated in Figure 9A.

It was shown that the incorporation of even a small amount of C18A into the physical QPA network structure leads to the formation of a macroscopic gel. For instance, in the presence of 2 mol% C18A (with respect to the monomers AMPS + APTAC), physical QPA hydrogels could be obtained at or above 1.0 M monomer concentration C_M , while without C18A, no gel could be obtained until C_M is increased to 2.5 M (Figure 10).⁶⁵ This highlights significant effect of the hydrophobic interactions between C18A segments on the onset of gelation. Hydrophobically modified QPA hydrogels containing 60% to 90% water exhibit a high tensile strength and stretchability of up to

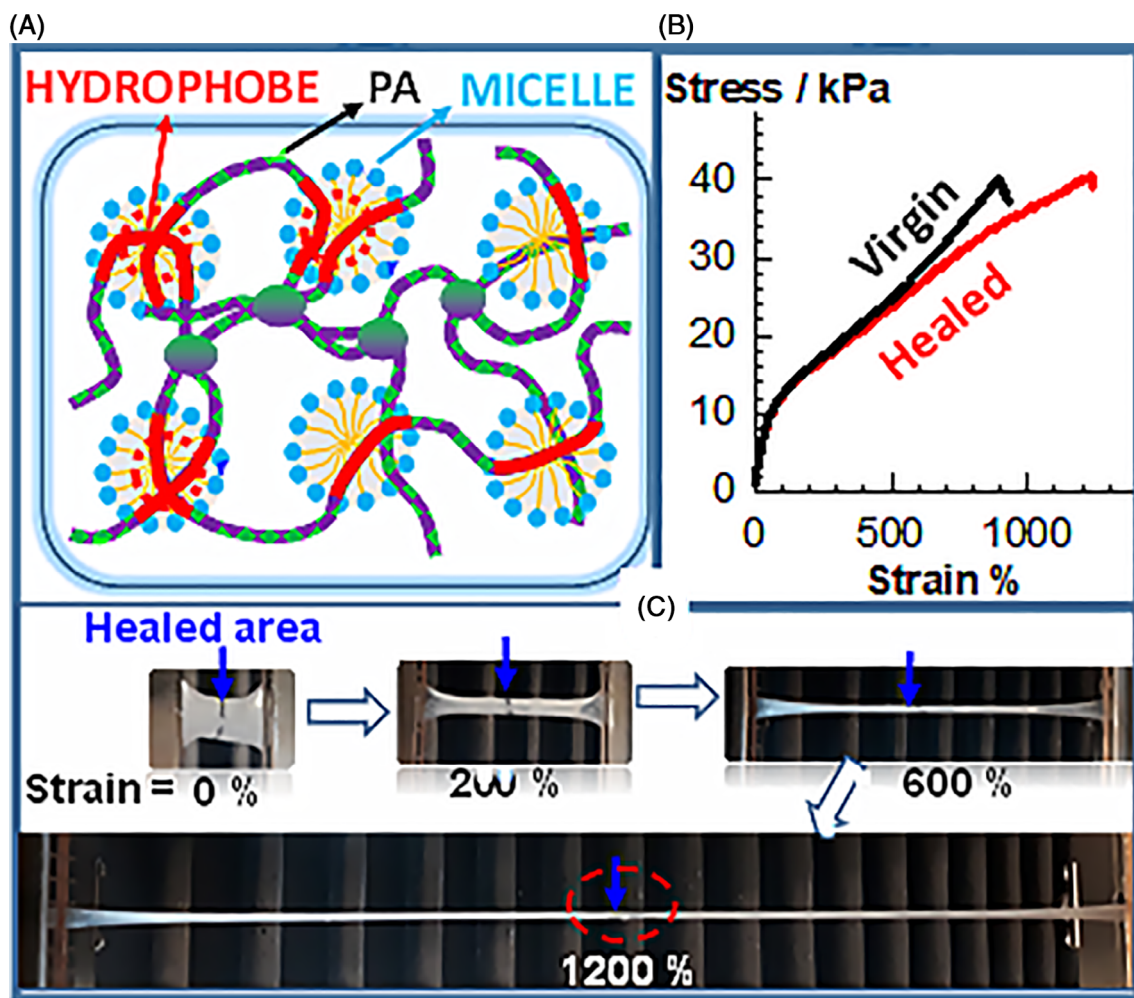


FIGURE 9 (A) Cartoon showing the structure of QPA hydrogels formed via micellar polymerization. The green balls represent ionic bonds between PA chains. (B) Typical stress–strain curves of QPA hydrogels with 5 mol% C18A before (black) and after healing at $50 \pm 2^\circ\text{C}$ for 24 hours (red). (C) Images of a healed hydrogel specimen with 5 mol% C18A during stretching. Healed area is indicated by arrows. The location of the fracture point is shown by the red dashed circle. Adapted from Reference 65 with permission from Springer Nature [Colour figure can be viewed at wileyonlinelibrary.com]

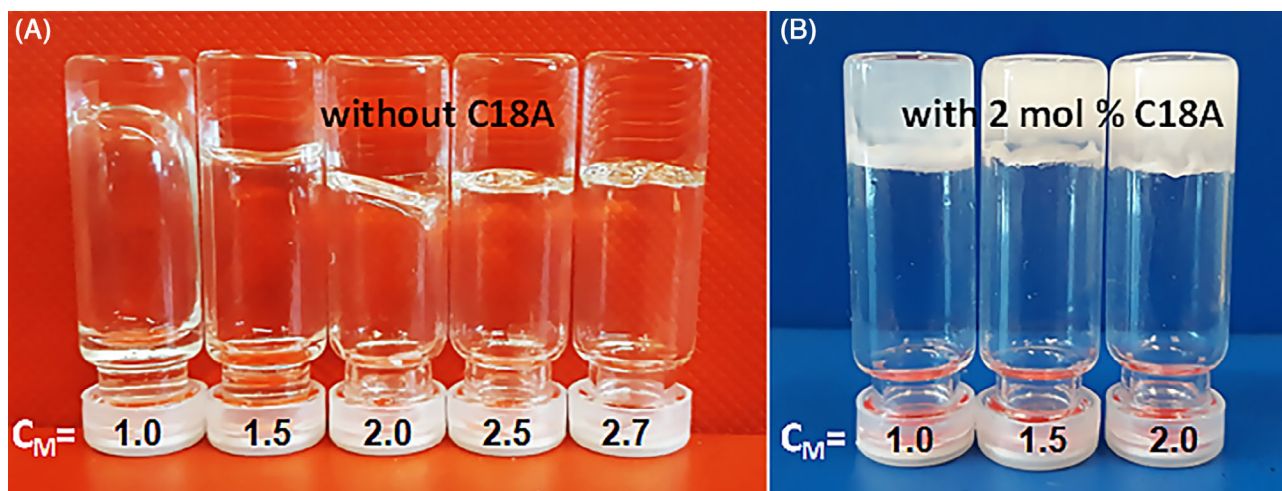


FIGURE 10 Images of QPA hydrogels based on AMPS and APTAC prepared at various C_M without (A) and with 2 mol% C18A (B). Reproduced from Reference 65 with permission from Springer Nature [Colour figure can be viewed at wileyonlinelibrary.com]

202 kPa and 1239%, respectively, that can be tuned by the amount of C18A as well as by the monomer concentration. Interestingly, QPA hydrogels equilibrium swollen in water are stiffer as compared to the as-prepared ones, which is in contrast to the theory of rubber elasticity as swelling decreases the cross-link density of gels. The authors explain this finding with the existence of SDS micelles in as-prepared hydrogels having the function of weakening the hydrophobic interactions.⁶⁵ Cut-and-heal tests revealed that all as-prepared hydrophobically modified QPA hydrogels exhibit healing behavior induced by heating.⁶⁵ For instance, the hydrogel with 5 mol% C18A shows a complete healing efficiency with respect to Young's modulus, tensile strength, and elongation at break after a healing time at $50 \pm 2^\circ\text{C}$ of 1 day (Figure 9B). Figure 9C presents images of a healed hydrogel specimen with 5 mol% C18A during stretching up to 1200% stretch ratio at which it fractures at any location in the middle as the virgin one.

4 | COMPLEXES OF QUENCHED POLYAMPHOLYTES

Formation of intra- and interpolyelectrolyte complexes with participation of polyampholytes was recently reviewed.⁶⁹ However, to the best of our knowledge the complexation of QPA with respect to high- and low-molecular-weight substances is a less studied topic. A pair of anionic diblock (AMPS_{50-co}-APTAC₅₀)₉₁-b-(AMPS)₆₇ and cationic diblock (AMPS_{50-co}-APTAC₅₀)₉₁-b-(APTAC)₈₈ copolymers, denoted as P(SA)₉₁S₆₇ and P(SA)₉₁A₈₈, respectively, were involved into complexation reaction to form stoichiometric PIC micelles (Figure 11).⁵⁸ The R_h values of the diblock copolymers separately in 0.1 M NaCl were 5.7 and 6.0 nm while the R_h of the PIC micelle thus formed increased to 29.0 nm suggesting that PIC micelle is spherical and consists of a core-shell structure where the anionic PAMPS and cationic PAPTAC blocks represent the core, and the amphoteric parts, P(SA)₉₁,

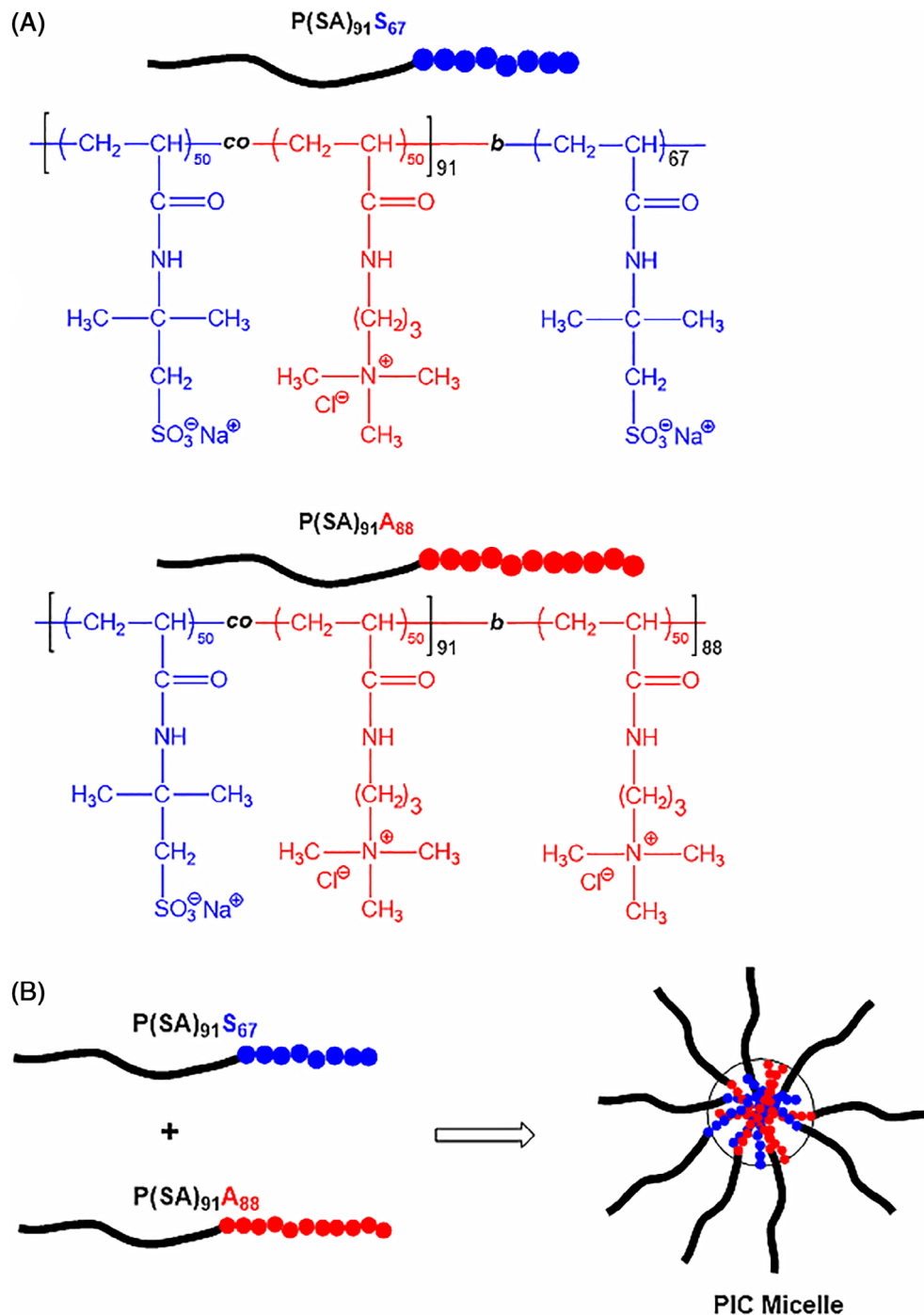
forms the shell. As revealed from zeta potential and TEM measurements the zeta-potential of PIC micelle was close to zero, the average radius of dried PIC was equal to 20.3 nm.

Analogously, mixing poly(2-(methacryloyloxy)ethyl phosphorylcholine)-b-PMAPTAC (PMPC-*b*-PMAPTAC) and poly(2-(methacryloyloxy)ethyl phosphorylcholine)-b-PAMPS (PMPC-*b*-PAMPS) leads to the spontaneous formation of core-shell PIC vesicles composed of PIC core and PMPC shells (Figure 12).¹¹ The hydrodynamic radius (R_h) and aggregation number (N_{agg}) of PICsomes in 0.1 M NaCl were equal to 78.0 nm and 7770, respectively. Since the PICsomes contain a spherical hollow covered by biocompatible PMPC shell, they may be useful for immobilization of bioactive compounds and controlled delivery to appropriate targets.

The complexation of charge unbalanced linear and cross-linked AMPS_{25-co}-APTAC₇₅ and AMPS_{75-co}-APTAC₂₅ copolymers was studied in aqueous solutions of surfactants and ionic dyes.⁴⁶ Complexations of AMPS_{25-co}-APTAC₇₅ with the anionic surfactant sodium dodecylbenzenesulfonate (SDBS), and AMPS_{75-co}-APTAC₂₅ with the cationic surfactant cetyltrimethyl ammonium chloride (CTMAC) are accompanied by changes in turbidity, zeta-potential and average hydrodynamic diameter of colloid particles. The optimal molar ratios of QPA-surfactant complexes are equal to $\sim 3:2$ and $\sim 2:3$ for [AMPS_{25-co}-APTAC₇₅]:[SDBS] and [AMPS_{75-co}-APTAC₂₅]:[CTMAC], respectively. It is obvious that SDBS binds to the positively charged APTAC while CTMAC to the negatively charged AMPS. In both cases, the surfactant molecules form intramolecular micelle structures surrounded by negatively or positively charged monomers. Complexation of AMPS-APTAC hydrogels with SDBS and CTMAC is accompanied by gradual shrinking of the gel samples because the anionic and cationic surfactants interact with excessive anionic and cationic groups of hydrogels. Gradually penetration of surfactant molecules inside hydrogel volume can lead to the formation of micelles within hydrogel matrix and hydrophobization of the whole system leading to the overall shrinkage of the hydrogel.

QPA hydrogels containing an excess of negative (AMPS-75H) and positive (AMPS-25H) charges effectively absorb methylene blue

FIGURE 11 Anionic diblock $P(SA)_{91}S_{67}$ and cationic diblock $P(SA)_{91}A_{88}$ copolymers (A) and formation of PIC micelle (B). Redrawn from Reference 58 with permission from MDPI [Colour figure can be viewed at wileyonlinelibrary.com]



(MB) and methyl orange (MO), respectively, due to electrostatic binding. However, in case of AMPS-50H, the oppositely charged chains compensate each other and both MB and MO molecules are not able to penetrate into the hydrogel matrix. Penetration of dye molecules inside of AMPS-25H and AMPS-50H hydrogel matrices proceeds via the race-relay ion transport, or ion-hopping transport mechanism, resulting in gel contraction.⁷⁰ Release of dye molecules from hydrogel matrix reached up to 70% to 75% in the medium of 0.5 M KCl. QPA composed of NaSS and VBTAC repeatedly absorbs bisphenol A at room temperature and release it at higher temperature, which is very

important for the removal of hydrophobic aromatic compounds from very dilute aqueous solutions.⁷¹

5 | APPLICATION ASPECTS OF QUENCHED POLYAMPHOLYTES

QPA hydrogels of high toughness, excellent bio- and hemocompatibility, anti-biofouling, self-healing ability, cytotoxic, and adhesive properties in physiological conditions are advanced to the

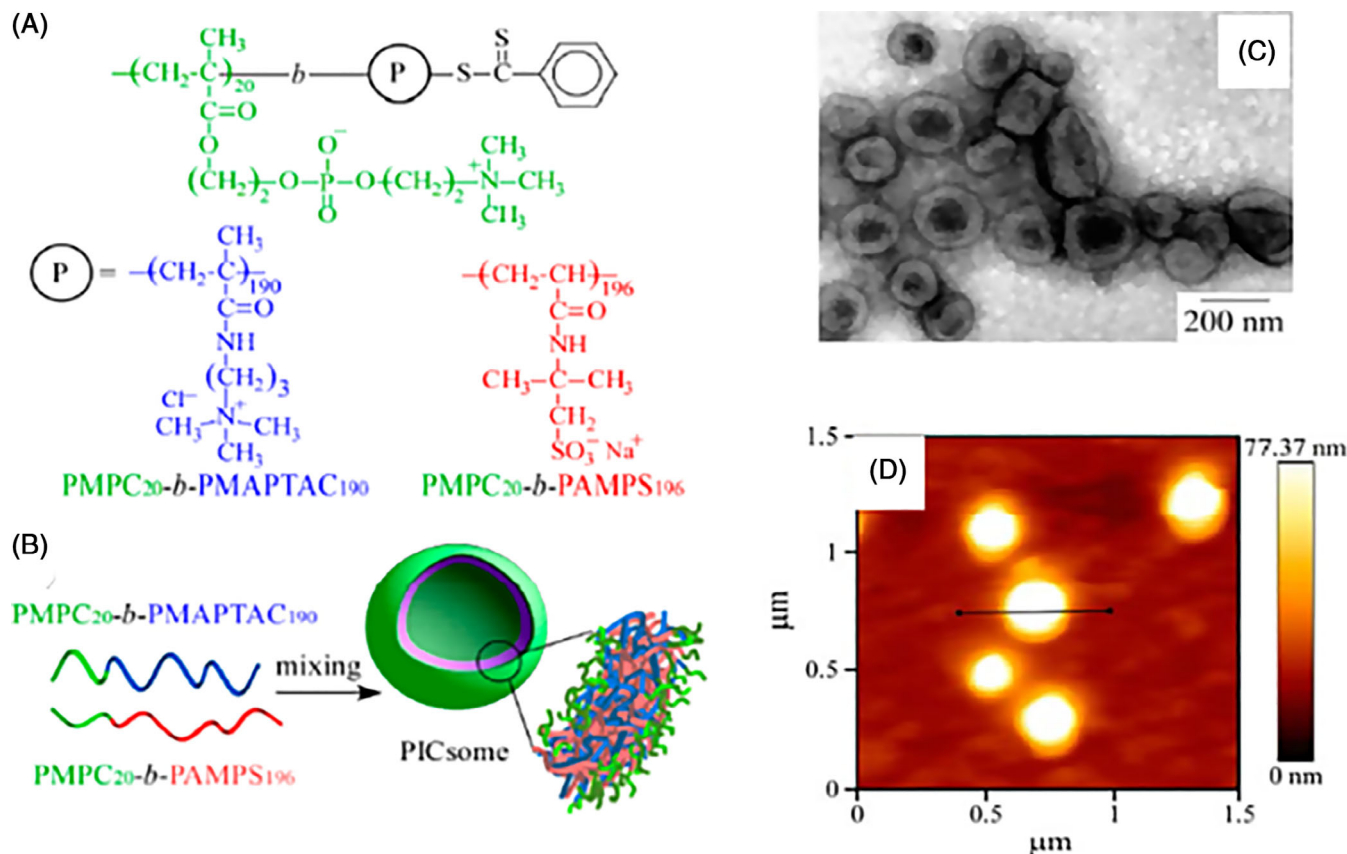


FIGURE 12 Chemical structures of oppositely charged diblock copolymers PMPC-*b*-PMAPTAC and PMPC-*b*-PAMPS (A), polyion complex vesicle (PICsome) composed of PMPC-*b*-PMAPTAC and PMPC-*b*-PAMPS (B), TEM (C), and AFM (D) images of vesicles. Reproduced from Reference 11 with permission from MDPI [Colour figure can be viewed at wileyonlinelibrary.com]

forefront of perspective structural biomaterials such as cartilage, anti-thrombogenic implants, wound dressings, blood-contacting materials, and drug delivery systems. Hemocompatibility of linear QPA made of 3-sulfopropylmethacrylate (SPMA) and METMAC at various molar ratios was evaluated with respect to human blood plasma in order to clarify the influence of charge balance (or imbalance) on plasma-protein association, blood-plasma clotting, and blood-cell hemolysis.⁶ The efficiency of SPMA-co-METMAC copolymers was compared with zwitterionic polymer polySBA (see Figure 8d). It was established that SPMA-co-METMAC copolymers with an excess of positive or negative charges enhance polyampholyte-protein associations. In contrast, the charge-balanced SPMA-co-METMAC copolymer and polySBA effectively resisted protein adsorption onto polymer interfaces and exhibited excellent nonfouling stability. These results suggest that the low protein-adsorption ability of equimolar SPMA-co-METMAC copolymer and polySBA is connected with overall charge neutrality of QPA. Moreover, both polySBA and charge-balanced SPMA-co-METMAC copolymer under physiological conditions showed very little hemolysis demonstrating good nonfouling nature and antihemolytic activity in relation to blood cell membranes. The best anticoagulant and antihemolytic activity of equimolar SPMA-co-METMAC copolymer is attributed to the formation of a highly hydrated layer formed between water molecules and anionic-cationic

groups. Thus, hemocompatible nature of SPMA-co-METMAC copolymer and polySBA has potential application to molecular design of tunable antithrombogenic materials for human blood. The adhesion and cytotoxicity tests of P(MAPTAC-co-NaSS) hydrogels were carried out with respect to fibroblast cells and macrophages.¹⁹ According to biomedical experiments the nontoxicity and excellent antifouling properties for polyampholyte hydrogels were observed toward macrophages. Barcellona et al²⁰ studied the drug release profile from a nonfouling polyampholyte hydrogel prepared from equimolar amounts of the cationic [2-(acryloyloxy)ethyl]trimethylammonium chloride (TMA) and anionic 2-carboxyethylacrylate (CAA) with triethyleneglycoldimethacrylate (TEGDMA) cross-linker in the presence of positively charged MB, negatively charged metanil yellow (MY) and neutral caffeine (C). The drug release kinetics of these three molecules from hydrogel matrix to the outer solution was studied as a function of cross-linker amount, pH of the solution, and salt concentration. It was shown that the drug release system is a promising platform for both short-term and long-term delivery of bioactive molecules.

Chung et al^{22,23} fabricated flexible, self-healing, cost-effective, and eco-friendly supercapacitors based on charge-balanced P(NaSS-MAPTAC) hydrogel and biochar, produced from the low-temperature pyrolysis of biological wastes, self-assembled with graphene oxide. At

room temperature, the supercapacitor shows a high energy density of 30 W h kg^{-1} with 90% capacitance retention after 5000 charge-discharge cycles at room temperature at a power density of 50 W h kg^{-1} . At a low temperature, -30°C , the supercapacitor exhibits an energy density of 10.5 W h kg^{-1} at a power density of 500 W h kg^{-1} .

Due to salt- and temperature resistance, QPA are widely applied in EOR as viscosifying and drag reduction agents where thickeners are required in brine solutions.^{18,25-32} Especially hydrophobically associating polyampholytes may be effective viscosity enhancers in high salinity media and temperature as they combine the self-assembly and polyampholyte properties.^{8,72-74} Application of hydrophobically modified and acrylamide-based polyampholytes in EOR was reviewed in detail recently.^{16,75} Low charge QPA containing acrylamide (90 mol%), AMPS (3-7 mol%), MADQUAT (3-7 mol%), and N,N-dihexylacrylamide or N-(4-ethylphenyl)acrylamide (0.5-1 mol%) exhibit improved thickening properties in comparison with unmodified polyampholytes containing 30 mol% AMPS and 70 mol% MADQUAT in high-salinity media.^{72,73} The viscosity of hydrophobically modified QPA increases much faster than that of unmodified one due to intermolecular association of hydrophobic parts. The viscosity of a 4 wt% hydrophobic polyampholyte solution in 1.5 M NaCl is 10^6 times higher than that of the unmodified one under identical conditions.

QPA in combination with surfactant can satisfy the harsh conditions of the deeper and hotter reservoirs and be applied for polymer flooding in EOR.⁷⁶ It was found that the interactions between the hydrophobically modified QPA and the C12/14 alkyl chains of surfactant result in the formation of mixed micelles serving as junction points for supramolecular network formation accompanied by a pronounced increase of the apparent solution viscosity. The salinity tolerance and thermal stability of QPA are suitable for application in high temperature and/or high-salinity reservoirs.⁷⁷ Equimolar QPA based on AMPS and APTAC dissolved in saline water with a mineralization of more than 200 g L^{-1} was tested to evaluate the flow behavior through porous media. It was found that approximately 80% of the injected QPA solution passes through the sand packed model without adsorption. This is due to the stable conformation of QPA demonstrating their applicability for EOR or tracer technology in saline water.

Aqueous solutions of QPA based on a copolymer composed of AAm, N,N-diallyl-N,N-dimethylammonium chloride, butyl acrylate, and AMPS units show enhanced apparent viscosity, viscoelasticity, thixotropy, controlled rheological properties and have a good potential for application in the clay-free and water-based drilling fluids.⁷⁸ The ability of QPA hydrogels to absorb saline water can be used for the production of drinking water.^{79,80} Moreover, QPA cryogels with a macroporous structure might be more suitable and cost-effective for desalination of saline water.

6 | CONCLUSION

The solution behavior of QPA is controlled by many parameters; among them, the copolymer composition and the ionic strength are the key factors. The charge-balanced QPA are poorly soluble or even

insoluble in pure water due to formation of intra- and interionic contacts between opposite charges that lead to overall hydrophobization of macromolecular chains and formation of colloidal particles or precipitates. However, they become soluble upon addition of low-molecular-weight salts due to disruption of intra- and interionic contacts demonstrating antipolyelectrolyte effect. Increase in the viscosity of linear QPA, or swelling of cross-linked QPA in salt solutions is an effective tool to develop viscosifying and drag reduction agents in high salinity reservoir for EOR and desalination technology. In case of charge-imbalanced QPA, they become water-soluble, and the hydrodynamic volume of the resulting solution increases in pure water due to electrostatic repulsion of positive or negative charges, while they both decrease upon addition of low-molecular-weight salts due to the polyelectrolyte effect. Charge-balanced and charge-imbalanced QPA can exist in core-shell state and exhibit antagonism in aqueous-salt solutions. Addition of low-molecular-weight salts will tend to shrink the shell part (polyelectrolyte region) and to swell the core part (polyampholyte region). Such antagonism between polyelectrolyte (shell) and polyampholyte (core) effects can take place at relatively high ionic strengths. The formation of intra- and interionic contacts is specific for QPA irrespective of the copolymer composition. The conformation of charge-balanced QPA in dilute solution or in gel state exists in a globular structure and is in good agreement with theoretical predictions. The QPA exhibit thermoresponsive character and display both LCST and UCST at certain salt and polymer concentrations and molecular weight of polymers. Introduction of hydrophobic groups to the macromolecular chain of QPA leads to self-assembling which is accompanied by a pronounced increase in the apparent solution viscosity. Such hydrophobically modified polyampholytes can serve as viscosifying agents in high salinity media and temperature. Supramolecular QPA prepared by random copolymerization of oppositely charged equimolar ionic monomers at a relatively high monomer concentration represents a new class of physical hydrogels containing both strong and weak ionic bonds. The former serves as permanent cross-links to maintain the shape of the gel while the latter as a sacrificial network responsible for high elongation, deformation, adhesion, self-healing, shape memory, and other important functions. The formation of stoichiometric polyionic complexes in the form of micelles and vesicles with core-shell structure is especially specific for diblock QPA. They are useful for embedding of bioactive substances and development of drug delivery systems. Linear and cross-linked charge-imbalanced QPA effectively absorb ionic dyes and surfactants while the charge-balanced QPA demonstrate excellent antifouling, anticoagulant, and antihemolytic activity in relation to blood cell membranes. QPA hydrogel electrolyte is promising to develop low temperature supercapacitors. The salt-tolerant and thermostable QPA together with hydrophobically modified QPA are suitable for application in EOR at harsh conditions and as drilling fluids. Accumulation of saline water by QPA hydrogels can be used for desalination and production of drinking water. For this purpose, the salt retaining property of macroporous QPA prepared under cryogenic conditions might be promising. Understanding of the fundamental relationships between the microstructure and property of linear and cross-linked amphoteric

macromolecules accompanied by systematic evaluation of literature sources will open renewed interest to polyampholytes in whole and QPA in particular.

ACKNOWLEDGEMENTS

This research was funded by the Science Committee of the Ministry of Education and Science of the Republic of Kazakhstan (Grant No. IRN AP08855552, 2018-2020). Sarkyt E. Kudaibergenov acknowledges Prof. Vitaliy V. Khutoryanskiy from the University of Reading (UK) for careful editing of the manuscript. Oguz Okay thanks the Türkiye Bilimler Akademisi (TUBA) for the partial support.

ORCID

Sarkyt E. Kudaibergenov  <https://orcid.org/0000-0002-1166-7826>

Oguz Okay  <https://orcid.org/0000-0003-2717-4150>

REFERENCES

1. Lowe AB, McCormick CL. Synthesis and solution properties of zwitterionic polymers. *Chem Rev.* 2002;102:4177-4189.
2. Dai C, Xu Z, Wu Y, et al. Design and study of a novel thermal-resistant and shear-stable amphoteric polyacrylamide in high-salinity solution. *Polymers.* 2017;9:296.
3. Sun TL, Luo F, Kurokawa T, Karobi SN, Nakajima T, Gong JP. Molecular structure of self-healing polyampholyte hydrogels analyzed from tensile behaviors. *Soft Matter.* 2015;11:9355-9366.
4. Sun TL, Luo F, Hong W, et al. Bulk energy dissipation mechanism for the fracture of tough and self-healing hydrogels. *Macromolecules.* 2017;50:2923-2931.
5. Ihsan AB, Sun TL, Kurokawa T, et al. Self-healing behaviors of tough polyampholyte hydrogels. *Macromolecules.* 2016;49:4245-4252.
6. Shih YJ, Chang Y, Quemener D, et al. Hemocompatibility of polyampholyte copolymers with well-defined charge bias in human blood. *Langmuir.* 2014;30:6489-6496.
7. Sponchioni M, Palmiero UC, Manfredini N, Moscatelli D. RAFT copolymerization of oppositely charged monomers and its use to tailor the composition of nonfouling polyampholytes with an UCST behavior. *React Chem Eng.* 2019;4:436-446.
8. Quan H, Li Z, Huang Z. Self-assembly properties of temperature- and salt-tolerant amphoteric hydrophobically associating polyacrylamide. *RSC Adv.* 2016;6:49281-49288.
9. Garnier T, Dochter A, Chau NTT, Schaaf P, Jierry L, Boulmedais F. Surface confined self-assembly of polyampholytes generated from charge-shifting polymers. *Chem Commun.* 2015;51:14092-14095.
10. Nakai K, Nishiuchi M, Inoue M, et al. Preparation and characterization of polyion complex micelles with phosphobetaine shells. *Langmuir.* 2013;29:9651-9661.
11. Nakai K, Ishihara K, Kappl M, Fujii S, Nakamura Y, Yusa S. Polyion complex vesicles with solvated phosphobetaine shells formed from oppositely charged diblock copolymers. *Polymers.* 2017;9:49-64.
12. Kawata Y, Kozuka S, Yusa S-I. Thermo-responsive behavior of amphoteric diblock copolymers bearing sulfonate and quaternary amino pendant groups. *Langmuir.* 2019;35:1458-1464.
13. Sharker KK, Ohara Y, Shigeta Y, Ozoe S, Yusa S-I. Upper critical solution temperature (UCST) behavior of polystyrene-based polyampholytes in aqueous solution. *Polymers.* 2019;11:265.
14. Zhang Q, Hoogenboom R. UCST behavior of polyampholytes based on stoichiometric RAFT copolymerization of anionic and cationic monomers. *Chem Commun.* 2015;51:70-73.
15. Wever DAZ, Picchioni F, Broekhuis AA. Polymers for enhanced oil recovery: a paradigm for structure-property relationship in aqueous solution. *Prog Polym Sci.* 2011;36:1558-1628.
16. Rabiee A, Amir E-L, Hajar J. Polyacrylamide-based polyampholytes and their applications. *Rev Chem Eng.* 2014;30:501-519.
17. Mumick PS, Welch PM, Salazar LC, McCormick CL. Water soluble copolymers 56. Structure and solvation effects of polyampholytes in drag reduction. *Macromolecules.* 1994;27:323-331.
18. Peiffer DG, Brunswick E, Lundberg RD, Kowalik RM, Turner SR. Drag reduction agents for aqueous salt solutions US Patent 4460758, 1984.
19. Sun TL, Kurokawa T, Kuroda S, et al. Physical hydrogels composed of polyampholytes demonstrate high toughness and viscoelasticity. *Nat Mater.* 2013;12:932-937.
20. Barcellona M, Johnson N, Bernards MT. Characterizing drug release from nonfouling polyampholyte hydrogels. *Langmuir.* 2015;31:13402-13409.
21. Xu S, Wu R, Huang X, Cao L, Wang J. Effect of the anionic-group/cationic group ratio on the swelling behavior and controlled release of agrochemicals of the amphoteric, superabsorbent polymer poly(acrylic acid-co-diallyldimethylammonium chloride). *J Appl Polym Sci* 2006;102:986-991.
22. Charaya H, Li X, Jen N, Chung H-J. Specific ion effects in polyampholyte hydrogels dialyzed in aqueous electrolytic solutions. *Langmuir.* 2019;35:1526-1533.
23. Li X, Wang X, Ok YS, Elliott JAW, Chang SX, Chung H-J. Flexible and self-healing aqueous supercapacitors for low temperature applications: polyampholyte gel electrolytes with biochar electrodes. *Sci Rep.* 2017;7:1685.
24. Zhang Y, Liao J, Sun W, Tong Z. Polyampholyte hydrogels with pH modulated shape memory and spontaneous actuation. *Adv Funct Mater.* 2018;28:1707245.
25. McCormick CL, Johnson CB. Water-soluble copolymers 28. Ampholytic copolymers of sodium 2-acrylamido-2-methylpropanesulfonate with (2-acrylamido-2-methylpropyl)dimethylammonium chloride: synthesis and characterization. *Macromolecules.* 1988;21:686-693.
26. Kathman EE, Salazar LC, McCormick CL. Copolymers of sodium 2-acrylamido-2-methylpropanesulfonate with (2-acrylamido-2-methylpropyl)trimethylammonium chloride. *Polym Prepr.* 1991;32:98-99.
27. McCormick CL, Salazar LC. Water soluble copolymers 43. Ampholytic copolymers of sodium 2-(acrylamido)-2-methylpropanesulfonate with 2-(acrylamido)-2-methylpropanetrimethylammonium chloride. *Macromolecules.* 1992;25:1896-1900.
28. McCormick CL, Salazar LC. Water soluble copolymers 44. Ampholytic terpolymers of acrylamide with sodium 2-acrylamido-2-methylpropanesulfonate and 2-acrylamido-2-ethylpropanetrimethylammonium chloride. *Polymer.* 1992;33:4384-4387.
29. McCormick CL, Salazar LC. Water soluble copolymers 45. Ampholytic terpolymers of acrylamide with sodium 3-acrylamido-3-methylbutanoate and 2-acrylamido-2-methylpropanetrimethylammonium chloride. *J Appl Polym Sci.* 1993;48:1115-1120.
30. Fevola MJ, Bridges JK, Kellum MG, Hester RD, McCormick CL. pH-responsive ampholytic terpolymers of acrylamide, sodium 3-acrylamido-3-methylbutanoate and (3-acrylamidopropyl)trimethylammonium chloride. I. Synthesis and characterization. *J Appl Polym Sci.* 2004;42:3236-3251.
31. Fevola MJ, Kellum MG, Hester RD, McCormick CL. pH-responsive ampholytic terpolymers of acrylamide, sodium 3-acrylamido-3-methylbutanoate and (3-acrylamidopropyl) trimethylammonium chloride. II. Solution properties. *J Appl Polym Sci.* 2004;42:3252-3270.
32. McCormick CL, Salazar LC. Water-soluble copolymers: 44. Ampholytic terpolymers of acrylamide with sodium 2-acrylamido-2-methylpropanesulfonate and 2-acrylamido-2-methylpropanetrimethylammonium chloride. *J Appl Polym Sci.* 2010;48:1115-1120.
33. Corpart JM, Candau F. Formulation and polymerization of microemulsions containing a mixture of cationic and anionic monomers. *Colloid Polym Sci.* 1993;271:1055-1067.

34. Corpart JM, Candau F. Characterization of high charge density ampholytic copolymers prepared by microemulsion polymerization. *Polymer*. 1993;34:3873-3886.
35. Corpart JM, Candau F. Aqueous solution properties of ampholytic copolymers prepared in microemulsions. *Macromolecules*. 1993;26:1333-1343.
36. Skouri M, Munch JP, Candau SJ, Neyret S, Candau F. Conformation of neutral polyampholyte chains in salt solutions: a light scattering study. *Macromolecules*. 1994;27:69-76.
37. Ohlemacher A, Candau F, Munch JP, Candau SJ. Aqueous solution properties of polyampholytes: effect of net charge distribution. *J Polym Sci Part B Polym Phys*. 1996;34:2747-2757.
38. Candau F, Joanny JF. Polyampholytes (properties in aqueous solution). In: Salamone JC, ed. *Polymeric Materials Encyclopedia*. Boca Raton, NY: CRC Press; 1996:5476-5488.
39. Nisato G, Munch JP, Candau SJ. Swelling, structure, and elasticity of polyampholyte hydrogels. *Langmuir*. 1999;15:4236-4244.
40. Salamone JC, Rice WC. Polyampholytes. In: Mark HF, Bikales NM, Overberger CG, Menges G, eds. *Encyclopedia of Polymer Science and Engineering*. New York: Wiley; 1987:514-530.
41. Laschewsky A. Structures and synthesis of zwitterionic polymers. *Polymers*. 2014;6:1544-1601.
42. Nakahata R, Yusa S. Solution properties of amphoteric random copolymers bearing pendant sulfonate and quaternary ammonium groups with controlled structures. *Langmuir*. 2019;35:1690-1698.
43. Fouillet CC, Greaves TL, Quinn JF, et al. Copolyampholytes produced from RAFT polymerization of protic ionic liquids. *Macromolecules*. 2017;50:8965-8978.
44. Delgado JD, Schlenoff JB. Static and dynamic solution behavior of a polyzwitterion using a Hofmeister salt series. *Macromolecules*. 2017;50:4454-4464.
45. Toleutay G, Shakhvorostov A, Kabdrakhmanova S, Kudaibergenov S. Solution behavior of "quenched" or strongly charged polyampholytes in aqueous-salt solutions. *Bull Karaganda Univ Chem Ser*. 2019;2:35-44.
46. Toleutay G, Dauletbekova M, Shakhvorostov A, Kudaibergenov S. Quenched polyampholyte hydrogels based on (3-acrylamidopropyl) trimethyl ammonium chloride and sodium salt of 2-acrylamido-2-methyl-1-propanesulfonic acid. *Macromol Symp*. 2019;385:1800160.
47. Kudaibergenov SE. Recent advances in studying of synthetic polyampholytes in solutions. *Adv Polym Sci*. 1999;144:115-197.
48. Kudaibergenov SE. *Polyampholytes: Synthesis, Characterization and Application*. New York: Kluwer Academic/Plenum Publishers; 2002 220 pp.
49. Kudaibergenov SE. Polyampholytes. *Encyclopedia of Polymer Science and Technology*. Hoboken, NJ: John Wiley Interscience; 2008:1-30.
50. Kudaibergenov S, Jaeger W, Laschewsky A. Polymeric betaines: synthesis, characterization and application. *Adv Polym Sci*. 2006;201:157-224.
51. Higgs PG, Joanny JF. Theory of polyampholyte solutions. *J Chem Phys*. 1991;94:1543-1554.
52. Everaers R, Johner A, Joanny JF. Complexation and precipitation in polyampholyte solutions. *Europhys Lett*. 1997;37:275-280.
53. Li X, Charaya H, Bernard GM, et al. Low-temperature ionic conductivity enhanced by disrupted ice formation in polyampholyte hydrogels. *Macromolecules*. 2018;51:2723-2731.
54. Li X, Charaya H, Tran TNT, Lee B, Cho J-Y, Chung H-J. Direct visualization of nano and microscale polymer morphologies in as-prepared and dialyzed hydrogels by electron microscopy techniques. *MRS Commun*. 2018;8:1079-1084.
55. Edwards SF, King PR, Pincus P. Phase change in polyampholytes. *Ferroelectrics*. 1980;30:3-6.
56. Dobrynin AV, Colby RH, Rubinstein M. Polyampholytes. *J Polym Sci Part B Polym Phys*. 2004;42:3513-3538.
57. Thivaios I, Kakogianni S, Bokias G. A library of quinoline-labeled water-soluble copolymers with pH-tunable fluorescence response in acidic region. *Macromolecules*. 2016;49:3526-3534.
58. Nakahata R, Yusa S. Preparation of water-soluble polyion complex (PIC) micelles covered by amphoteric random copolymer shells with pendant sulfonate and quaternary amino groups. *Polymers*. 2018;10:205.
59. Su E, Okay O. Polyampholyte hydrogels formed via electrostatic and hydrophobic interactions. *Eur Polym J*. 2017;88:191-204.
60. Luo F, Sun TL, Nakajima T, et al. Strong and tough polyion-complex hydrogels from oppositely charged polyelectrolytes: a comparative study with polyampholyte hydrogels. *Macromolecules*. 2016;49:2750-2760.
61. Gao M, Gawel K, Stokke BT. Polyelectrolyte and antipolyelectrolyte effects in swelling of polyampholyte and polyzwitterionic charge balanced and charge offset hydrogels. *Eur Polym J*. 2014;53:65-74.
62. Tierney H, Hjelme DR, Stokke BT. Determination of swelling of responsive gels with nanometer resolution. Fiber-optic based platform for hydrogels as signal transducers. *Anal Chem*. 2008;80:5086-5093.
63. Wang F, Yang J, Zhao J. Understanding anti-polyelectrolyte behavior of a well-defined polyzwitterion at the single chain level. *Polym Int*. 2015;64:999-1005.
64. Gong JP. Why are double network hydrogels so tough? *Soft Matter*. 2010;6:2583-2590.
65. Toleutay G, Su E, Kudaibergenov S, Okay O. Highly stretchable and thermally healable polyampholyte hydrogels via hydrophobic modification. *Colloid Polym Sci*. 2020;298:273-284.
66. Hill A, Candau F, Selb J. Properties of hydrophobically associating polyacrylamides: influence of the method of synthesis. *Macromolecules*. 1993;26:4521-4532.
67. Tuncaboylu DC, Sarı M, Oppermann W, Okay O. Tough and self-healing hydrogels formed via hydrophobic interactions. *Macromolecules*. 2011;44:4997-5005.
68. Can V, Kochovski Z, Reiter V, et al. Nanostructural evolution and self-healing mechanism of micellar hydrogels. *Macromolecules*. 2016;49:2281-2287.
69. Kudaibergenov SE, Nuraje N. Intra- and interpolyelectrolyte complexes of polyampholytes. *Polymers*. 2018;10:1146.
70. Kabanov VA. Polyelectrolyte complexes in solution and condensed phase. *Uspekhi Khimii (Russ Chem Rev)*. 2005;74:5-23.
71. Morisada S, Suzuki H, Emura S, Hirokawa Y, Nakano Y. Temperature-swing adsorption of aromatic compounds in water using polyampholyte gel. *Adsorption*. 2008;14:621-628.
72. Kujawa P, Rosiak JM, Selb J, Candau F. Synthesis and properties of hydrophobically modified polyampholytes. *Mol Cryst Liq Cryst*. 2000;354:401-407.
73. Kujawa P, Rosiak JM, Selb J, Candau F. Micellar synthesis and properties of hydrophobically associating polyampholytes. *Makromol Chem Phys*. 2001;202:1384-1397.
74. El-hoshoudy AN, Desouky SEM, Elkady MY, Alsabagh AM, Betiha MA, Mahmoud S. Investigation of optimum polymerization conditions for synthesis of cross-linked polyacrylamide-amphoteric surfer nanocomposites for polymer flooding in sandstone reservoirs. *Int J Polym Sci*. 2015;2015:318708.
75. Kudaibergenov S, Koetz J, Nuraje N. Nanostructured hydrophobic polyampholytes: self-assembly, stimuli-sensitivity, and application. *Adv Compos Hybrid Mater*. 2018;1:649-684.
76. Liu R, Pu W, Wang L, et al. Solution properties and phase behavior of a combination flooding system consisting of hydrophobically amphoteric polyacrylamide, alkyl polyglycoside and n-alcohol at high salinities. *RSC Adv*. 2015;5:69980-69989.
77. Mukhametgazy N, Gussenov I, Shakhvorostov A. Quenched polyampholytes for polymer flooding. *AIP Conf Proc*. 2019;2167:020236.

78. Zhang X, Jiang G, Xuan Y, Wang L, Huang X. Associating copolymer acrylamide/diallyldimethylammonium chloride/butyl acrylate/2--acrylamido-2-methylpropanesulfonic acid as a tackifier in clay-free and water-based drilling fluids. *Energy Fuels*. 2017;31:4655-4662.
79. Fosso-Kankeu E, Varachia H, Waanders F. Reduction of salinity of water using acrylamide-based polyampholyte. 10th International Conference on Advances in Science, Engineering, Technolnolgy and Healthcare (ASETH-18); November 19-20, 2018; Cape Town, South Africa.
80. Ekici S. Thermoresponsive crosslinked ampholytic terpolymers (CATs): effect of salt concentration on porosity, thermal, mechanical,

electrical conduction, and imprintable properties. *J Mater Sci Nanotechnol*. 2019;7:1-11.

How to cite this article: Kudaibergenov SE, Okay O. Behaviors of quenched polyampholytes in solution and gel state. *Polym Adv Technol*. 2020;1-16. <https://doi.org/10.1002/pat.5112>